ELSEVIER

International Journal of Solids and Structures 41 (2004) 131–143

INTERNATIONAL JOURNAL OF SOLIDS and STRUCTURES

www.elsevier.com/locate/ijsolstr

Modelling of dynamic behaviour of concrete materials under blast loading

Yong Lu *, Kai Xu

School of Civil and Environmental Engineering, Nanyang Technological University, 50 Nanyang Avenue, Block N1, 1a-29, Singapore 639798, Singapore

Received 3 April 2003; received in revised form 10 September 2003

Abstract

In order to model the behaviour of concrete structures under blast loading, it is essential to be able to model the dynamic strength and other strain rate dependent properties of the concrete material. In this paper, a constitutive model for predicting the dynamic strength and damage of concrete subjected to blast loading is developed. The model stems from the continuum fracture mechanics of microcrack nucleation, growth and coalescence to formulate the evolution of damage. The concrete is assumed as homogeneous continuum with pre-existing microcracks. Damage to concrete is defined as the probability of fracture at a given crack density, obtained by integrating a crack density function over time. Based on the damage function, the stress response at a particular time, and hence the dynamic stress–strain relationship, can be established for a given strain-rate. The required material constants representing initial crack properties are derived from material dynamic strength tests. Comparison with available test results shows that the proposed model can give consistent prediction of the dynamic behaviour of concrete materials. Nominal fragment sizes of concrete and fracture strain energy are also derived which can be useful in an energy-based concrete break-up and debris throw prediction procedure.

Keywords: Concrete; Fracture; Fragmentation; Strain rate; Dynamic strength

1. Introduction

The possibility of accidental explosions is present wherever explosives are stored. Of particular concern over the harmful physical effects of an accident is the concrete debris throw, which can be a governing factor on the safe siting distance of aboveground ammunition magazines and other explosives storage facilities. Experimental and analytical studies in recent years have led to the development of some conceptual and empirical approaches for the prediction of initial debris parameters and debris throw distance. However, these approaches have limited applications due to the fact that they do not involve physical

* Corresponding author. Tel.: +65-6790-5272; fax: +65-6791-0676.
E-mail address: cylu@ntu.edu.sg (Y. Lu).

0020-7683/$ - see front matter © 2003 Elsevier Ltd. All rights reserved.
doi:10.1016/j.ijsolstr.2003.09.019

modeling of the process of material breakup and the formation of fragmentation. In order to bridge this gap, modeling the constitutive dynamic behaviour of concrete material under high loading rate is necessary.

Under blast loading, the concrete damage and fragmentation result from both impulsive loading by stress waves and gas-driven fracture propagation. Studies (Simha et al., 1987; Hommert et al., 1987; Brinkman, 1987) tend to support the view that stress waves generated by the detonation of an explosive charge are responsible for the development of damage zone in the concrete material and the subsequent fragment size distribution, while the explosion gases are important in the separation of a crack pattern that has already been formed during the passage of the stress wave, and in the subsequent launch of the fragments. Fragment formation is deemed to be a much slower process than the propagation of the stress wave; however, there is evidence that the fragment size is determined immediately after the passage of the stress wave and long before the gas penetration and throw movement take place (Brinkman, 1987; Zhao et al., 1993). The findings by Wilson (1987) suggest that the information about fragment size distribution during shock loading is important since the majority of fragments are formed in this stage. In other words, the fragment formation is under very high loading rate; hence, the strain-rate effect on material properties plays an important role in the breakup and fragmentation process.

Concrete is a typical brittle material and its dynamic behaviour is strain-rate dependent. As with most brittle materials, such strain-rate dependence may be derived from evolution of damage based on fracture mechanics. This paper presents a model for damage and fracture of concrete and mortar materials under dynamic loading. In the model, the concrete is assumed in a macroscopic view as homogeneous continuum with pre-existing microcracks. The evaluation of damage is formulated based on the continuum fracture mechanics of microcrack nucleation, growth and coalescence. Based on the damage function, the stress response at a particular time, and hence the stress–strain relationship, can be established for a given strain-rate. The required material constants representing initial crack properties can be derived from material dynamic property tests. Comparison with available test results shows that the proposed model can give consistent prediction of the dynamic behaviour of concrete materials. The nominal fragment sizes of concrete and fracture strain energy are also derived.

2. A continuum model for damage and fracture of concrete materials

When the loading rate is high, the mechanical response of a material is generally different from that at a low loading rate. Such rate dependence is observed for nearly all the brittle materials (Clifton, 2000). Concrete exhibits also an enigmatic phenomenon of increased resistance when it is loaded at a very high rate.

Generally speaking, the total energy, U, for a brittle body subjected to some external surface traction and undergoing crack development can be expressed as

$$U = U_0 + U_c + U_k \tag{1}$$

where U_0 is the elastic strain energy which can be obtained through integration of stress or strain (rate dependent) in the body, U_c is the surface energy necessary for the formation of crack surfaces in the body, which can be obtained by introducing a cohesive crack model, and U_k is the kinetic energy in the system due to fragment motions. For the evaluation of fracture and formation of fragments, the elastic strain energy will be critical.

In some early continuum models for brittle materials (Grady and Kipp, 1980; Taylor et al., 1980; Kuszmaul, 1987), it is assumed that microcracks initiate and grow immediately when the strain becomes tensile. In more recent studies (Zhang et al., 2001; Liu and Katsabanis, 1997), a critical strain value was proposed based on the experimental observation that brittle materials (such as rock) do not fail at tensile stresses below their static tensile strength. It was demonstrated that the use of the critical value makes it

possible to obtain a stable solution which confirms the theory of explosive energy partitioning in brittle materials. This consideration is also adopted in the present study of concrete materials.

Experimental results have indicated that the dynamic Young's modulus of concrete increases with strain rate in the very high strain rate regime (e.g. 100 s^{-1} and higher) (Grote et al., 2001; Tedesco and Ross, 1998). An appropriate theory to explain this phenomenon is yet to be established. In the present study, the dynamic Young's modulus is assumed to vary with strain rate in an exponential function based on available test results. Thus, considering the degrading effect at fracture, the dynamic Young's modulus, E_d, can be written as

$$E_d = e^{a\sqrt[3]{\dot{\varepsilon}}+b\sqrt[3]{\dot{\varepsilon}^2}E(1-D)} \tag{2}$$

where E is the Young's modulus for the undamaged virgin material under quasistatic loading, D is a damage scalar, $\dot{\varepsilon}$ is the strain rate, a and b are constants which can be evaluated from test data, and $e^{a\sqrt[3]{\dot{\varepsilon}}+b\sqrt[3]{\dot{\varepsilon}^2}} \geqslant 1$. The elastic strain energy for the damaged material subject to a uniaxial stress (Jean, 1991) can therefore be expressed in a modified form as

$$U_0 = \tfrac{1}{2}e^{a\sqrt[3]{\dot{\varepsilon}}+b\sqrt[3]{\dot{\varepsilon}^2}E(1-D)\varepsilon^2} \tag{3}$$

where ε is a uniaxial strain that depends on the material and loading rate, U_0 is the elastic strain energy. Thermodynamic restrictions require that the tensile stress σ be given by

$$\sigma = \frac{\partial U_0}{\partial \varepsilon} = e^{a\sqrt[3]{\dot{\varepsilon}}+b\sqrt[3]{\dot{\varepsilon}^2}E(1-D)\varepsilon} \tag{4}$$

It is not possible to describe the contribution of each microcrack in degrading the material stiffness. However, with the development in statistical fracture mechanics, the damage scalar D may be defined in terms of the volume of idealized penny-shaped cracks in the material as (Grady and Kipp, 1980)

$$D = NV \tag{5}$$

where N is the number of cracks per unit volume or crack density, $V = \frac{4}{3}\pi r^3$ is the spherical region surrounding the penny-shaped crack of radius r that approximates the stress-relieved volume due to the traction-free boundary of the crack. For isotropic damage, D varies in the range of 0–1, with $D = 0$ corresponding to the virgin material without damage, and $D = 1$ corresponding to the initiation of macrocrack. Intermediate values of D correspond to the partially damaged material.

As mentioned before, considering the fact that certain time duration is needed for fracture to take place when a brittle material like concrete is subjected to a stress higher than its static strength (Zhang et al., 2001), the evolution of damage can be determined by the number of cracks activated at the time t as follows:

$$D(t) = \int_{t_c}^{t} \dot{N}(s)V(t-s)\,ds \tag{6}$$

where t_c is the time duration needed for the tensile strain ε to reach the critical value ε_{cr}. For uniaxial tension, $\varepsilon_{cr} = \sigma_{st}/E$, with σ_{st} being the static tensile strength. $\dot{N}$ is the crack density increment. According to Yang et al. (1996),

$$\dot{N} = \alpha(\varepsilon - \varepsilon_{cr})^{\beta} \tag{7}$$

where α is used to describe the nucleation of the microcracks at a certain strain level. β is material constant which determines the stain rate dependence of crack density increment. Obviously the crack density increment vanishes if the tensile strain $\varepsilon \leqslant \varepsilon_{cr}$.

The volume $V(t-s)$ can be determined by a microstructure law to correspond to the growth of cracks that are activated at past time, s,

$$V(t-s)=\frac{4}{3}\pi r^3=\frac{4}{3}\pi c_g^3(t-s)^3 \tag{8}$$

where c_g is the crack growth velocity and generally $0<c_g<c_l$, with c_l being the elastic wave speed (Miller et al., 1999). Substituting Eqs. (7) and (8) into Eq. (6), a general expression for the damage growth can be obtained

$$D(t)=\frac{4}{3}\alpha\pi c_g^3\int_{t_c}^{t}(\varepsilon-\varepsilon_{cr})^{\beta}(t-s)^3\,\mathrm{d}s \tag{9}$$

Assuming a constant strain rate $\dot{\varepsilon}_0$, and hence $\varepsilon(t)=\dot{\varepsilon}_0 t$, the expression for damage growth becomes

$$D(t)=\frac{4}{3}\alpha\pi c_g^3\dot{\varepsilon}_0^{\beta}\int_{t_c}^{t}(s-t_c)^{\beta}(t-s)^3\,\mathrm{d}s=m\dot{\varepsilon}_0^{\beta}(t-t_c)^{\beta+4} \tag{10}$$

where

$$m=\frac{8\pi c_g^3\alpha}{(\beta+1)(\beta+2)(\beta+3)(\beta+4)} \tag{11}$$

The dynamic fracture strength is defined as the maximum stress in a material before failure due to fracture. With the assumption of constant strain loading rate, from Eqs. (4) and (10), it has

$$\sigma=\mathrm{e}^{a\sqrt[3]{\varepsilon_c}+b\sqrt[3]{\varepsilon_c^2}}E\dot{\varepsilon}_0 t\quad\text{for } t\leqslant t_c \tag{12}$$

$$\sigma=\mathrm{e}^{a\sqrt[3]{\varepsilon_c}+b\sqrt[3]{\varepsilon_c^2}}E\dot{\varepsilon}_0 t[1-m\dot{\varepsilon}_0^{\beta}(t-t_c)^{\beta+4}]\quad\text{for } t_c<t\leqslant t_m \tag{13}$$

Eq. (13) can be differentiated with respect to time. Subsequently, the time instant t_m that corresponds to the maximum stress can be determined by setting the differentiation equal to zero, and hence the following equation

$$m\dot{\varepsilon}_0^{\beta}(t_m-t_c)^{\beta+3}[t_m-t_c+t_m(\beta+4)]=1 \tag{14}$$

The value of β and m for a particular brittle material such as concrete can be evaluated from the dynamic strength test data. Once β and m are available, the dynamic stress–strain relationship can be determined according to Eqs. (12) and (13).

The higher dynamic strength at higher strain rates is consistent with the observed test results. Rate effects leads to higher strength but the failure process becomes more brittle. The post-peak failure becomes more unstable and the mechanism with which the material behaves at this stage significantly differs from the pre-peak response. According to Reinhardt et al. (1990) and Mindess (1983), there is a process zone of microcracking ahead of the tip of the macrocrack of concrete material. During the crack propagation, the energy barriers delay the total failure of material. Consequently the heterogeneity affects the shape of the softening zone considerably. This observation agrees with the experimental results reported by Shah and John (1986) and Yon et al. (1991).

Herein a cohesive crack model is used to model the material softening process. Cohesive crack will be formed in the direction normal to the maximum primary stress when the maximum primary stress reaches $\bar{\sigma}_m$. The stress on the microcrack surface is related to the nominal strain. The normal stress σ is a decreasing function of strain, and the surface where $0<\varepsilon<\bar{\varepsilon}$, is called process zone or craze. σ vanishes when the normal strain is larger than the material parameter $\bar{\varepsilon}$, which represents a nominal cohesive strain limit, and the surface when $\varepsilon>\bar{\varepsilon}$ is called macrocrack. On the macrocrack, no interaction is assumed between the two surfaces, i.e., $\sigma=0$. If the cohesive strain increases from 0 to $\bar{\varepsilon}$, the energy change will be equal to $\int_0^{\bar{\varepsilon}}\sigma\,\mathrm{d}\varepsilon=G_{cI}$. In case of a linear variation of cohesive stress and strain, the area of the triangle $\zeta=\frac{1}{2}\bar{\sigma}_m\bar{\varepsilon}$

denotes energy change per unit crack length from cohesive crack into opened crack. σ is the stress that can be developed by cohesive crack model. This can be expressed mathematically by

$$\Phi = \sigma - (\bar{\sigma}_{\mathrm{m}} + \bar{h}\varepsilon) \leqslant 0 \tag{15}$$

$$\varepsilon' \geqslant 0, \quad \Phi\varepsilon' = 0 \tag{16}$$

where $\bar{h} = -\bar{\sigma}_{\mathrm{m}}/\bar{\varepsilon}$, $\bar{\sigma}_{\mathrm{m}}$ is the maximum dynamic stress occurring at time t_{m}, $\bar{\varepsilon}$ is a material parameter representing a nominal dynamic cohesive strain limit. $\bar{h}$ indicates the craze hardening modulus which is negative for softening. The pointed symbol denotes the increment. Based on the research by Weerheijm (1992) regarding the softening of concrete under tension, the dynamic cohesive strain limit $\bar{\varepsilon}$ can be expressed by

$$\bar{\varepsilon} = \bar{\varepsilon}_{\mathrm{sy}} \cdot \left(\frac{\dot{\varepsilon}}{\dot{\varepsilon}_{\mathrm{s}}}\right)^{-0.042} \tag{17}$$

where $\dot{\varepsilon}_{\mathrm{s}}$ is a reference static strain rate and here it is taken to be $\dot{\varepsilon}_{\mathrm{s}} = 4 \times 10^{-6}\ \mathrm{s}^{-1}$, $\bar{\varepsilon}_{\mathrm{sy}}$ is the nominal static cohesive strain limit for concrete and according to Holmquist et al. (1993), $\bar{\varepsilon}_{\mathrm{sy}} = 0.01$. The dynamic softening curve can therefore be expressed as

$$\sigma = \bar{\sigma}_{\mathrm{m}} \cdot \left[1 - \left(\frac{\varepsilon - \bar{\varepsilon}_{\mathrm{m}}}{\bar{\varepsilon}}\right)^{k}\right] \quad t > t_{\mathrm{m}} \tag{18}$$

where $\bar{\varepsilon}_{\mathrm{m}}$ is the critical strain at the dynamic maximum stress. k can be determined by fitting to the experimental post-peak softening curve.

Based on the dynamic strength of the concrete material established earlier, the fragmentation can be evaluated by applying the method proposed for rock materials (Grady and Kipp, 1980; Zhang et al., 2001), as follows. It is known that fragments are associated with crack initiation, propagation and coalescence. Thus, it is necessary to know the crack size in order to predict the fragment size. Hence, the damage defined by Eq. (6) is expressed in terms of the distribution of crack size as

$$D(t) = \int_0^{c_{\mathrm{g}}(t-t_{\mathrm{c}})} \omega(r,t)\mathrm{d}r \tag{19}$$

where

$$\omega(r,t) = \frac{4\pi r^3}{3c_{\mathrm{g}}}\alpha\dot{\varepsilon}_0^{\beta}(t - t_{\mathrm{c}} - r/c_{\mathrm{g}})^{\beta} \tag{20}$$

is the damage or crack volume fraction distribution. r is the penny shaped crack radius.

Fragmentation is deemed to occur when the stress reaches the material dynamic strength $\bar{\sigma}_{\mathrm{m}}$, which corresponds to time t_{m}. At fracture coalescence, the fracture faces form the fragment sizes. Noting that the crack radius $r = L/2$ with L being the nominal fragment size, the fragment size distribution can be obtained as follows:

$$F(L) = \frac{1}{2}\omega(L/2, t_{\mathrm{m}}) \tag{21}$$

Substituting Eq. (20) into Eq. (21) yields

$$F(L) = \frac{\pi\alpha L^3}{12c_{\mathrm{g}}}\dot{\varepsilon}_0^{\beta}[t_{\mathrm{m}} - t_{\mathrm{c}} - L/(2c_{\mathrm{g}})]^{\beta} \tag{22}$$

To determine the strain rate dependence of the dominant fragment size (fragment size corresponding to the largest volume fraction of material), the fragment size distribution $F(L)$ can be maximized with respect to the fragment size L. It is found that the fragment size distribution $F(L)$ has a maximum when

$$L_{\mathrm{m}} = \frac{6c_{\mathrm{g}}}{\beta+3}(t_{\mathrm{m}} - t_{\mathrm{c}}) \tag{23}$$

This expression describes the strain rate dependence of the dominant fragment size.

3. Energy formulation

The strain energy of material upon fracture coalescence can be written as

$$U_0 = \int_V u\,\mathrm{d}V = \int_V \int_0^{t_{\mathrm{m}}} \sigma\,\mathrm{d}\varepsilon\,\mathrm{d}V \tag{24}$$

in which the strain energy density

$$\begin{aligned} u &= \int_0^{t_{\mathrm{m}}} \sigma\,\mathrm{d}\varepsilon = \int_0^{t_{\mathrm{c}}} E\dot{\varepsilon}_0^2 t\,\mathrm{d}t + \int_{t_{\mathrm{c}}}^{t_{\mathrm{m}}} E\dot{\varepsilon}_0^2[1 - m\dot{\varepsilon}_0^{\beta}(t-t_{\mathrm{c}})^{\beta+4}]t\,\mathrm{d}t \\ &= \frac{1}{2}E\dot{\varepsilon}_0^2 t_{\mathrm{m}}^2 + \frac{Em\dot{\varepsilon}_0^{\beta+2}}{(\beta+5)(\beta+6)}\left(t_{\mathrm{m}} - \frac{\sigma_{\mathrm{st}}}{E\dot{\varepsilon}_0}\right)^{\beta+6} - \frac{1}{\beta+5}Em\dot{\varepsilon}_0^{\beta+2}t_{\mathrm{m}}\left(t_{\mathrm{m}} - \frac{\sigma_{\mathrm{st}}}{E\dot{\varepsilon}_0}\right)^{\beta+5} \end{aligned} \tag{25}$$

The fracture softening strain energy can be described as

$$U_{\mathrm{c}} = \int_V u_{\mathrm{c}}\,\mathrm{d}V = \int_V \int_{\bar{\varepsilon}_{\mathrm{m}}}^{\bar{\varepsilon}+\bar{\varepsilon}_{\mathrm{m}}} \sigma\,\mathrm{d}\varepsilon\,\mathrm{d}V \tag{26}$$

in which the strain energy density

$$u_{\mathrm{c}} = \int_{\bar{\varepsilon}_{\mathrm{m}}}^{\bar{\varepsilon}+\bar{\varepsilon}_{\mathrm{m}}} \sigma\,\mathrm{d}\varepsilon = \frac{1}{2}\bar{\sigma}_{\mathrm{m}}(\bar{\varepsilon}+2\bar{\varepsilon}_{\mathrm{m}})\bar{\varepsilon} - \frac{1}{k+1}\bar{\sigma}_{\mathrm{m}}\bar{\varepsilon}\bar{\varepsilon}_{\mathrm{m}} - \frac{1}{k+2}\bar{\sigma}_{\mathrm{m}}\bar{\varepsilon}^2 \tag{27}$$

The kinetic energy of debris can be obtained from Eq. (1)

$$U_{\mathrm{k}} = U - U_0 - U_{\mathrm{c}} \tag{28}$$

where U is the input total energy, U_0 is the elastic strain energy and U_{c} is fracture softening strain energy. Subsequently, the debris throw velocity can be determined.

4. Modeling results

The above described theoretical procedure is applied to model the dynamic behaviour of concrete materials in conjunction with pertinent experimental data. The experimental results used to derive the material parameters include concrete and mortar under tensile and compressive loading. The mortar is regarded as representing the matrix phase of concrete. Based on the test data, the parameters a and b in Eq. (2) are evaluated to be $a = -0.08502$ and $b = 0.01441$ and the corresponding dynamic Young's modulus function curve is shown in Fig. 1. It is noted that the initial dynamic Young's modulus values are taken at a stress level immediately below the quasistatic strength. The damage is considered equal zero at this stage under dynamic loading.

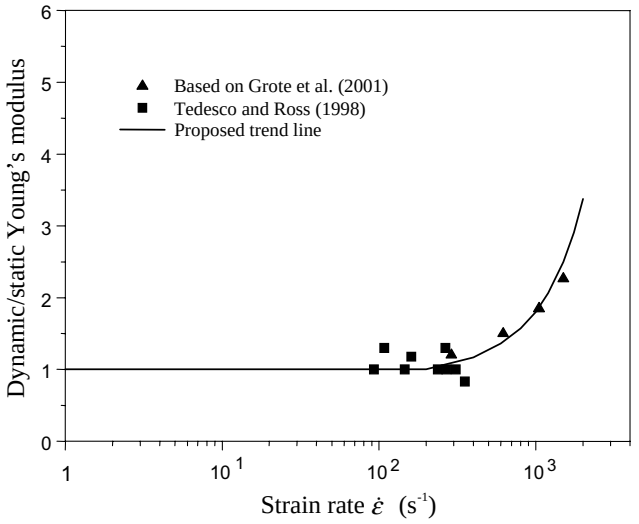

Fig. 1. Variation of Young's modulus with strain rate.

The measured dynamic strength and static strength data are employed to evaluate the material constants β and m according to Eq. (14). The results are then applied in the theoretical model to predict the dynamic strength and establish the dynamic stress–strain relationships for the materials under varying strain loading rate, as well as the fragment size and the fracture strain energy.

It should be pointed out that the damage in concrete under compression essentially is also related to crack growth and coalescence; therefore, the basic model developed in the previous section is also implemented for concrete/mortar materials under compression. In this respect, however, the value of t_c ought to be determined according to the quasistatic compressive strength instead of the tensile strength, while the static nominal cohesive strain limit, which in the case of compression implies the compressive strain corresponding to lateral fracture, is taken to be $\bar{\varepsilon}_{sy} = 0.01/v \approx 0.01/0.18 = 0.05$, where v is the Poisson's ratio.

4.1. Concrete under tension

In the dynamic tests of concrete material under tension and compression reported in (Tedesco et al., 1993; Ross et al., 1995), the concrete material had a quasistatic tensile strength $\sigma_{st} = 3.86$ MPa, Young's modulus $E = 27$ GPa, and mass density $\rho = 2400$ kg/m^3. Poisson's ratio is estimated to be $v = 0.18$. Fig. 2 shows the measured dynamic to (quasi) static strength ratio as a function of the logarithmic strain rate (the strain rate for the quasistatic strength is on the order of 10^{-6}–10^{-5}). Based on these data, the material constants are evaluated to be $\beta = 10$, and $m = 8.1 \times 10^{49}$ according to Eq. (14). With these values, the dynamic stress–strain relationship at a given strain rate $\dot{\varepsilon}$ can be established using Eqs. (12), (13) and (18). Fig. 3 shows the resulting dynamic stress–strain relationship for concrete under tension for various constant strain rates. The predicted dynamic strength to static strength ratios are compared with the test results in Fig. 2, whereby some other test results outside those used for the evaluation of β and m are also included (Weerheijm, 1992; Ross et al., 1995). It can be observed that the predicted values agree very well with the collective experimental data. As can be seen, at a strain rate of order of 10 s^{-1}, the dynamic tensile strength of concrete increases to 3–4 times of the static tensile strength; and at strain rate of 100 s^{-1}, the increase reaches about 7.

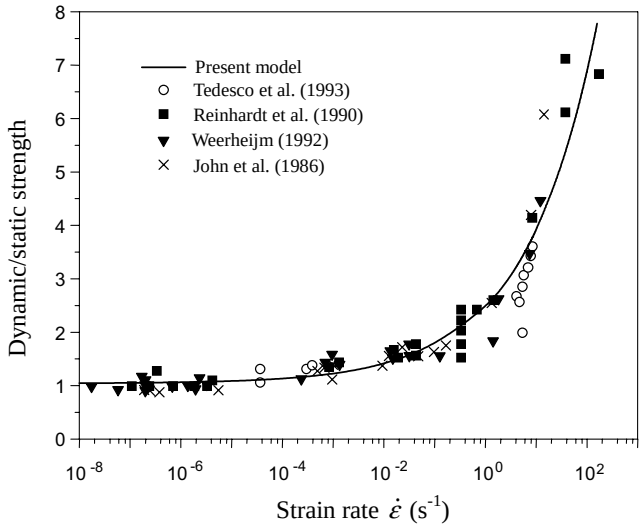

Fig. 2. Normalized dynamic concrete tensile strength vs. strain rate.

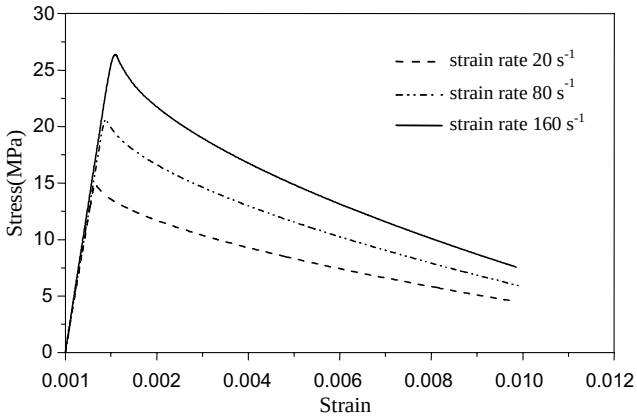

Fig. 3. Predicted stress–strain curves for concrete under tension with different strain rates.

4.2. Concrete under compression

The concrete material for dynamic compression tests used for the evaluation of β and m had the same static material properties as mentioned in the previous section. The nominal quasistatic compressive strength from the various specimens was about 40 MPa. Fig. 4 shows the measured dynamic compressive strength against the strain rate. By fitting the test data with Eq. (14), the material parameters β and m are found to be $\beta = 10$, and $m = 7.42 \times 10^{47}$. Subsequently, the predicted dynamic compressive strength can be obtained based on Eq. (13) and they are shown with the test data in Fig. 4. The predicted stress–strain relationship of concrete under compression is compared with experimental results obtained by Donze et al. (1999) in Fig. 5. A favourable agreement is observed.

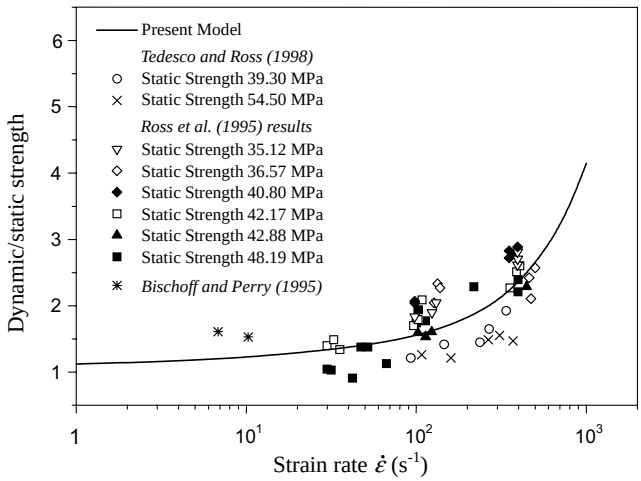

Fig. 4. Normalized concrete compressive strength vs. strain rate.

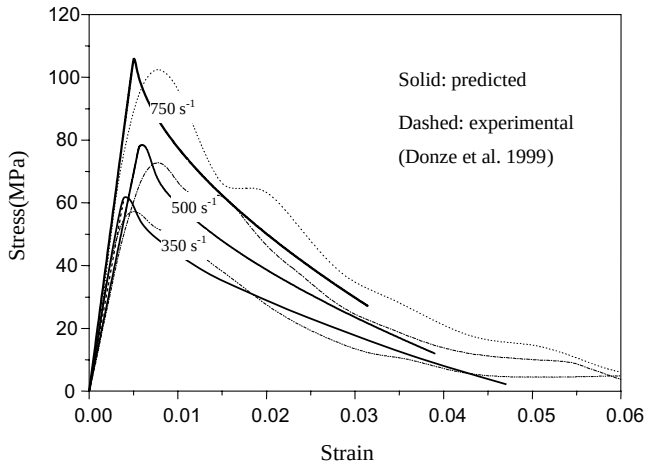

Fig. 5. Compressive stress–strain relationships of concrete at different strain rates.

Comparing to the rate enhancement on the dynamic tensile strength, the strain rate effect on the dynamic compressive strength appears to be much less significant. At a strain rate of order of 100 s^{-1}, the dynamic compressive strength is about 1.5 times of the static compressive strength as compared to the tensile strength increase of 7 times at the same strain rate. However, it is interesting to note that if the rate enhancement is to be viewed in terms of the absolute strength increase, then the increases of strength under tension and comparison are actually comparable.

4.3. Mortar under compression

The mortar specimens tested by Grote et al. (2001) under compression are considered. The mortar material had static Young's modulus $E = 20$ GPa and a quasistatic compressive strength of approximately 46 MPa (Tedesco and Ross, 1998). The Poisson's ratio is estimated at $v = 0.2$, and mass density $\rho = 2100$ kg/m^3.

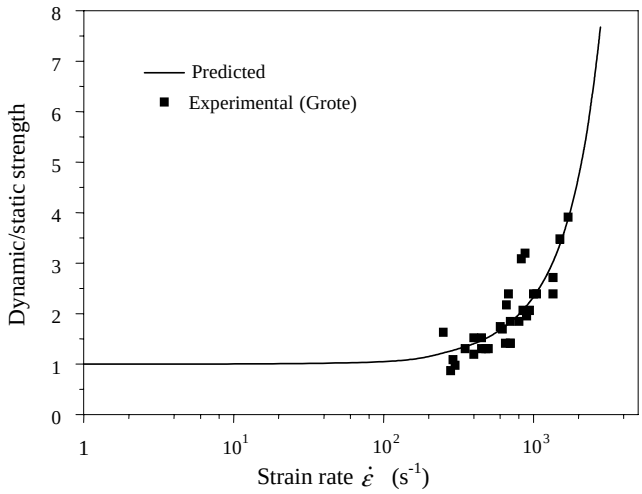

Fig. 6. Normalized mortar compressive strength vs. strain rate.

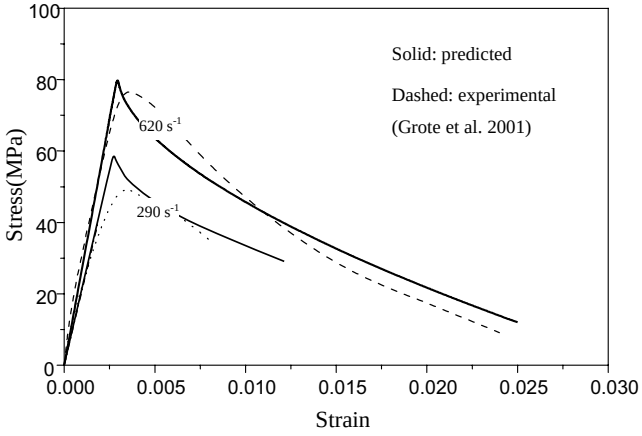

Fig. 7. Compressive stress–strain relationships of mortar at different strain rates.

The measured dynamic failure stress, shown in Fig. 6, increases with the strain rate in a similar manner as for concrete.

Based on the measured dynamic strength data, the material parameters β and m for mortar under compression are found to be $\beta = 7$, and $m = 3.16\times10^{44}$. The modelling results of the dynamic strength using these β and m values are depicted in solid line in Fig. 6. Furthermore, the predicted dynamic stress–strain relationships are compared with the available stress–strain curves from the mortar tests in Fig. 7. The predicted stress–strain curves agree favourably with the experimental results.

4.4. Fragmentation and fracture strain energy

Having obtained the β and m values, the fragment size can be calculated using Eq. (23) as a function of strain rate. For this purpose, an estimation of the damage growth rate needs to be given. A reasonable

estimate of damage growth rate during the dynamic fracture is about 0.4 times the longitudinal wave velocity (Grady and Kipp, 1980). The longitudinal wave velocity can be calculated according to the elastic theory from the mass density, Young's modulus and the Poisson's ratio. Thus, for the concrete under consideration the longitudinal wave velocity is calculated to be $c_l = 3495$ m/s, and hence the damage growth rate $c_g = 0.4c_l = 1398$ m/s; for mortar, $c_l = 3253$ m/s and $c_g = 1301.2$ m/s. Subsequently, the fragment sizes for concrete and mortar are calculated and the results are depicted in Fig. 8(a). As can be seen, the fragment size decreases with the increase of strain rate, as expected. The fragment size is on the order of 10 mm at a strain rate of 100 s^{-1}.

The fracture strain energy for concrete and mortar can also be determined by integrating the dynamic stress–strain curves, according to Eqs. (24) and (26). Fig. 8(b) shows the fracture strain energy density as a function of strain rate. The fracture strain energy density increases with increasing strain rate. The increasing rate of fracture energy is higher for concrete as compared with mortar. This may be attributed to the contribution of large size aggregates in the concrete. Under high rate loading, the presence of aggregate in the material could act to delay the crack propagation and coalescence, resulting in higher gain at high strain rate than mortar.

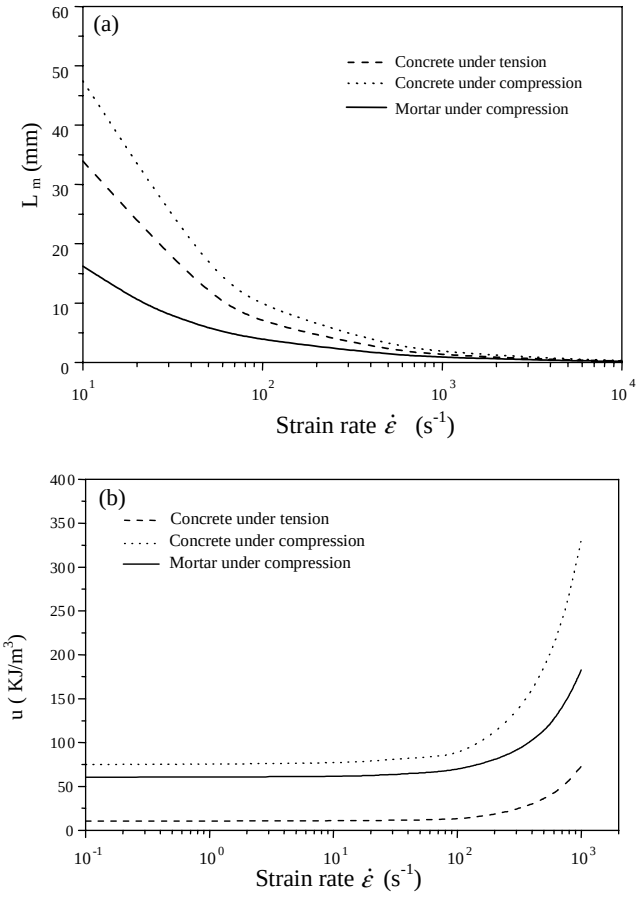

Fig. 8. Predicted fragment size and fracture energy vs. strain rate for concrete and mortar: (a) fragment size vs. strain rate, (b) fracture energy vs. strain rate.

5. Conclusions

A constitutive model for predicting the dynamic behaviour of concrete materials has been formulated based on continuum fracture theory of microcrack nucleation, growth and coalescence. With respect to experimental observation of increasing dynamic Young's modulus at very high strain rate, an empirical relationship of dynamic Young's modulus to the strain rate is incorporated into the model. The model is applied to concrete and mortar materials and the results are found to be consistent with the experimental data. For the class of materials considered in the modelling examples, the material constants β and m are found to be $\beta = 10$, $m = 8.1\times10^{49}$ for concrete under tension; $\beta = 10$, $m = 7.42\times10^{47}$ for concrete under compression; and $\beta = 7$, $m = 3.16\times10^{44}$ for mortar under compression. The subsequent dynamic stress–strain relationships and the predicted dynamic strengths are found to agree favourably the experimental results. Based on the β and m values, the fragment size distribution and fracture energy with varying strain rate are also obtained. The model provides a new perspective regarding the dynamic behaviour of concrete-like composite materials under high rate explosive loading.

The proposed model should be valid for all strain rate range. However, since the model parameters pertaining to the concrete materials (in particular β and m) are derived based on the experimental data at relatively high strain rate, it is recommended that the predicted dynamic stress–strain curves be considered for high loading rate applications with strain rate in a range of 1–1000/s, as may typically be encountered in the case of concrete materials under blast loading.

References

Bischoff, P.H., Perry, H., 1995. Impact behavior of plain concrete loaded in uniaxial compression. J. Eng. Mech. 121, 685–693.

Brinkman, J.R., 1987. Separating shock wave and gas expansion breakage mechanisms. In: Proceedings of the Second International Symposium on Rock Fragmentation by Blasting, Colorado, Keystone, pp. 6–15.

Clifton, R.J., 2000. Response of materials under dynamic loading. Int. J. Solids Struct. 37, 105–113.

Donze, F.V., Magnier, S.A., Daudeville, L., Mariotti, C., Davenne, L., 1999. Numerical study of compressive behavior of concrete at high strain rates. J. Eng. Mech. 125, 1154–1163.

Grady, D.E., Kipp, M.E., 1980. Continuum modelling of explosive fracture in oil shale. Int. J. Rock Mech. Min. Sci. Geomech. Abstr. 17, 147–157.

Grote, D.L., Park, S.W., Zhou, M., 2001. Dynamic behaviour of concrete at high strain rates and pressures: I. Experimental characterization. Int. J. Impact Eng. 25, 869–886.

Holmquist, T.J., Johnson, G.R., Cook, W.H., 1993. A computational constitutive model for concrete subjected to large strains, high strain rates, and high pressures. In: 14th International Symposium on Ballistics, Quebec, Canada, 26–29 September, pp. 591–600.

Hommert, P.J., Kuszmaul, J.S., Parrish, R.L., 1987. Computational and experimental studies of the role of stemming in cratering. In: Proceedings of the Second 2nd International Symposium on Rock Fragmentation by Blasting, Colorado, Keystone, pp. 550–562.

Jean, L., 1991. A Course on Damage Mechanics. Springer.

John, R., Shah, S.P., Jeng, Y.S., 1986. A fracture mechanics model to predict the rate sensitivity of Mode I fracture of concrete, Northwestern University, Evanston.

Kuszmaul, J.S., 1987. A new constitutive model for fragmentation of rock under dynamic loading. In: Proceedings of the Second International Symposium on Rock Fragmentation by Blasting, Colorado, Keystone, pp. 412–423.

Liu, L., Katsabanis, P.D., 1997. Development of a continuum damage model for blasting analysis. Int. J. Rock Mech. Min. Sci. 34, 217–231.

Miller, O., Freund, L.B., Needleman, A., 1999. Modelling and simulation of dynamic fragmentation in brittle materials. Int. J. Fract. 96, 101–125.

Mindess, S., 1983. The application of fracture mechanics to cement and concrete: a historical review. In: Wittmann, F.H. (Ed.), Fracture Mechanics of Concrete. Elsevier Science Publishers, Amsterdam.

Reinhardt, H.W., Rossi, P., Mier van, J.G.M., 1990. Joint investigation of concrete at high rates of loading. Mat. Struct. Res. Test. 23, 213–216.

Ross, C.A., Tedesco, J.W., Kuennen, S.T., 1995. Effects of strain rate on concrete strength. ACI Mater. J. 92, 37–47.

Shah, S.P., John, R., 1986. Strain rate effects on Mode I crack propagation in concrete. In: Wittmann, F.H. (Ed.), Fracture Toughness and Fracture Energy of Concrete. Elsevier Science Publishers, Amsterdam.

Simha, K.R.Y., Fourney, W.L., Dick, R.D., 1987. An investigation of the usefulness of stemming in crater blasting. In: Proceedings of the Second International Symposium on Rock Fragmentation by Blasting, Colorado, Keystone, pp. 591–599.

Taylor, L.M., Chen, E.P., Kuszmaul, J.S., 1980. Microcrack induced damage accumulation in brittle rock under dynamic loading. Comput. Meth. Appl. Mech. Eng. 55, 301–320.

Tedesco, J.W., Ross, C.A., 1998. Strain-rate-dependent constitutive equations for concrete. J. Press. Vess. Tech. 120, 398–405.

Tedesco, J.W., Ross, C.A., Kuennen, S.T., 1993. Experimental and numerical analysis of high strain rate splitting tensile tests. ACI Mater. J. 90, 162–169.

Weerheijm, J., 1992. Concrete under impact tensile loading and lateral compression. Doctoral thesis, TNO Prins Maurits Laboratory.

Wilson, W.H., 1987. An experimental and theoretical analysis of stress wave and gas pressure effects in bench-blasting. Ph.D. dissertation, University of Maryland.

Yang, Y., Bawden, W.F., Katsabanis, P.D., 1996. A new constitutive model for blast damage. Int. J. Rock Mech. Min. Sci. 33, 245–254.

Yon, J.H., Hawkins, N.M., Kobayashi, A.S., 1991. Fracture process zone in dynamically loaded crack-line wedge-loaded, double cantilever beam concrete specimen. ACI Mater. J. 88, 470–479.

Zhang, Y., Hao, H., Zhou, Y., 2001. A continuum model for dynamic damage and fragmentation of brittle solids. In: Proceedings of the Fourth Asia-pacific Conference on Shock and Impact Loads on Structures, Singapore, pp. 565–572.

Zhao, Y., Huang, J., Wang, R., 1993. Fractal characteristics of mesofractures in compressed rock specimens. Int. J. Rock Mech. Min. Sci. Geomech. Abstr. 30, 877–882.